This document is the Accepted Manuscript version of a Published Work that appeared in final form in Chem. Mater. **2016**, *28*, 207-213 *copyright © American Chemical Society after peer review and technical editing by the publisher. To access the final edited and published work see*
http://pubs.acs.org/doi/abs/10.1021/acs.chemmater.5b03902

Decreasing Charge Losses in Perovskite Solar Cells Through the mp-TiO_2/MAPI Interface Engineering.

Jose Manuel Marin-Beloqui,[1] Luis Lanzetta[1] and Emilio Palomares*[1,2]

[1]Institute of Chemical Research of Catalonia (ICIQ). The Barcelona Institute of Science and Technology. Avda. Països Catalans, 16. Tarragona. E-43007. Spain

[2]ICREA. Passeig Lluís Companys, 23. Barcelona. E-08010. Spain.

KEYWORDS: Pervoskite, Solar cells, charge transfer, interface

Based on our experience on controlling the recombination kinetics in Dye Sensitized Solar Cells (DSSC) through the modification of the mesoporous TiO_2 (mp-TiO_2) interface we have carried out the modification of the methyl ammonium lead iodide (MAPI) /mp-TiO_2 interface with a nanoscopic layer of insulating Al_2O_3. The effects over the device efficiency, Voc device reproducibility and the relationship between the observed increase in open-circuit voltage (Voc) and the presence of the Al_2O_3 layer is thoroughly discussed and explained. In contrast with the experimental observation in DSSC of TiO_2 conduction band edge shift for Al_2O_3 coated mp-TiO_2 films, in MAPI perovskite solar cells the charge vs voltage measurements carried out under sun-simulated irradiation conditions results in a negligible shift of the exponential charge distribution either measured using PICE (Photo Induced Charge Extraction) or PIDC (Photo Induced Differential Charging). Furthermore, an important decrease on the charge recombination lifetime is measured for the Al_2O_3 treated samples which lead to an improvement of the overall device efficiency due to the slower rate in the back-electron transfer reactions

.

Introduction.

The use of methyl ammonium lead iodide (MAPI) perovskite-type semiconductor material has been the focus of increase interest for the development of efficient solar cells[1-3]. In less than 5 years solar-to-electrical conversion efficiency have been increased from η=3.8% [4]efficiencies to near 20%[5], exceeding the top best efficiencies measured for other so-called third-generation solar cells such as DSSC[6] (Dye Sensitized Solar Cells), OSC[7] (Organic Solar Cells) and QDSC[8] (Quantum Dot Solar Cells). The easy-to-fabricate procedures, materials low cost and past experience on the above mentioned solar cell technologies have paved the way for MAPI solar cells to become a *hot spot* in materials science for energy conversion devices such as solar cells and light-emitting diodes[9]. Moreover, the recent discovery of the use of MAPI as semiconductor for solar cells, has also presented novel scientific challenges as for example, the explanation of the unusual large amount of measured charge on MAPI solar cells[10], the presence of hysteresis effects[11-14], the bi-exponential nature of the registered small-perturbation based Voc decays[15, 16] and/or the presence of interfacial dipoles[17, 18]. Whilst, the increase in solar cell efficiency has been spectacular, with a learning-curve never seen for other solar cell technologies alike CdTe and CIS, among others[19], the knowledge, however, on the detailed mechanisms that allows the efficient conversion of sun-light into electrical current have been less explored with remarkable exceptions[16, 20-23] and, moreover, there is still the scientific challenge to approach MAPI solar cells to their maximum theoretical efficiency through the reduction of non-radiate charge recombination losses[24], better spectral response[25] and , moreover, increasing operational stability[26].

One particular issue of MAPI perovskite solar cells is that the semiconductor thin film can be used in different device configurations as for example: (a) the use of mesoporous metal oxide scaffolds alike Al_2O_3, TiO_2 or ZnO[27]

as contacts, (b) without the mesoporous scaffold and (c) using organic materials as selective contacts[28]. Nonetheless, it is worthy to mention that the best certified devices have been described, to the best of our knowledge, with the archetypal device configuration[5] of FTO/d-TiO_2/mp-TiO_2/MAPI/HTM/Au where FTO is the fluorine doped tin oxide semiconductor layer deposited on glass, d-TiO_2 is a thinner (~50nm) dense layer of TiO_2, mp-TiO_2 is a thin mesoporous layer (~450nm) and the HTM is the organic hole transport material. The choice of metal contact is usually gold (Au) on this class of device architecture too.

For the reasons given below the above described device configuration is the standard used in this work unless otherwise stated: On the one hand, our experience on the deposition of the TiO_2 metal oxide[29], its characterization and previous encouraging results in relation with this work using this device structure[15] and, on the other hand, to clarify further the role on the mp-TiO_2 layer in the MAPI perovskite solar cell.

It is well known that reducing the charge losses due to inconvenient interfacial charge recombination reactions under operation is paramount to increase the solar cell efficiency[30]. Learning from past studies in DSSC, we have observed that direct back-electron transfer from the photo-injected electrons at the mp-TiO_2 to the oxidized electrolyte was a major issue to overcome to increase the solar cell efficiency. Indeed, reducing this particular charge recombination reaction through better dye design and rational interface engineering lead to better and more reproducible DSSC[31].

In our first communication using the MAPI perovskite semiconductor in solar cells[15], we hypothesized that several interfacial and band to band recombination pathways can be found in MAPI/mp-TiO_2/HTM sample as illustrated in Scheme 1. For one, after electron injection from the MAPI to the TiO_2 conduction band (reaction 3, Scheme 1) subsequent interfacial back electron transfer may takes place (reaction 6, Scheme 1). For another, the photo-injected electrons at the TiO_2 can also recombine with holes at the oxidized HTM (analogously to the reaction occurring in solid-state DSSC but it his case cannot be a direct recombination as there is a thin layer of MAPI perovskite between the TiO_2 and the HTM) and as measured by Moser and co-workers using laser transient absorption spectroscopy[20], (reaction 5, Scheme 1). Moreover, electrons at the MAPI perovskite can also recombine with the holes at the oxidized HTM (reaction 4, Scheme 1). Last but not least, band to band non-radiate and radiate charge recombination reactions at the MAPI perovskite (reaction 2 and 1, Scheme 1) have to be also considered as well as possible charge recombination reactions between electrons at the MAPI and surface states at the TiO_2 (reaction 7, Scheme 1).

Hence, the modification of the mp-TiO_2/MAPI perovskite interface may affect at least one of the recombination pathways that limit the solar cell performance.

The use of conformally deposited insulating overlayers onto the TiO_2 nanocrystals surface have been previously explored by our group and others in DSSC[32-34]. Indeed, it has been demonstrated that the interfacial engineering onto the semiconductor nanocrystals, either TiO_2 or ZnO, leads to a substantial decrease of the charge losses due to interfacial recombination processes. In fact, a recent publication[35] by Jung and co-workers describes the use of MgO onto mp-TiO_2 in MAPI solar cells, however, the device electronic characterization to understand the changes in solar cell Voc remained unclear.

In the present work we have fabricated MAPI perovskite solar cells with the archetypal structure mentioned above as well as MAPI perovskite solar cells with an Al_2O_3 insulating thin layer onto the nanocrystalline TiO_2 particles that conform the mp-TiO_2 layer. The former will be described along this work as MAPI perovskite solar cells, while the latter will be designed as Al_2O_3-coated perovskite solar cells. Moreover, we have used advanced photo-induced characterisation techniques, namely photo-induced transient photo-voltage (PIT-PV), photo-induced differential charging (PIDC) and photo-induced transient photo-current (PIT-PC) to thoroughly analyse the differences in charge density (defined as the total accumulated charge in the device at a given bias), the charge recombination lifetime and the relationship between both mentioned parameters. The findings described below are key to (a) understand further the device charge recombination processes that hamper the solar-to-electrical conversion efficiency and (b) to increase the device fabrication reproducibility through interface engineering.

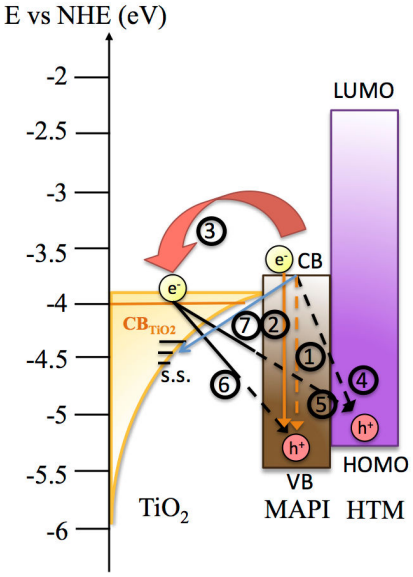

Scheme 1. The photo-induced interfacial charge transfer recombination reactions in MAPI perovskite solar cells; (1) band to band radiate recombination, (2) band to band non radiate recombination, (3) interfacial electron transfer from MAPI conduction band (CB) to TiO_2 and (4) interfacial electron transfer from the MAPI CB to the HTM, (5) interfacial electron transfer from TiO_2 CB to the HTM, (6) interfacial electron transfer from the TiO_2 CB to the MAPI and (7) interfacial electron transfer from the MAPI CB to TiO_2 surface states (s.s.).

Experimental Section.

Device preparation.

The FTO (Fluorine doped Tin Oxide) coated glasses (resistance= 8Ω/cm²) were etched using Zn powder (Alfa Aesar 98%) and a 2 M solution of HCl according to the desired pattern. Afterwards, the substrates were cleaned for 15 minutes in an ultrasound bath with de-ionized water with Hellmax soap, with de-ionized water and

finally with ethanol. The substrates were dried and an UV/Ozone treatment was performed for 20 minutes.

A solution of 0.65 mL of Ti (IV) isopropoxide (Sigma Aldrich 97%) and 0.38 mL of acetylacetone (Sigma Aldrich) were mixed in 5 mL of ethanol. This solution was spun-casted at 3000 rpm for 60s over the FTO. The substrates were calcined at 500ºC for 30 min to obtain the titanium oxide dense layer. Afterwards, titanium oxide-coated substrates were immersed in a 40 mM $TiCl_4$ solution at 70ºC for 30 minutes. Then, substrates were cleaned with water and ethanol and heated at 390ºC for 20 minutes.

A mixture of TiO_2 paste (Ti Nanoxide HT/SP Solaronix) and ethanol 2:5 (w:w) was spin-coated at 5000 rpm for 30 seconds. The substrates were heated at 325ºC for 30 min, 375ºC for 5 min, 450ºC for 15 min and 500ºC for 30 min. The substrates were heated at 500 ºC for 20-30 minutes prior to their use for further steps.

The alumina coating step was followed as previously reported by Palomares et al., in brief 3 mL of 3 M $Al(secbut)_3$ (Sigma Aldrich©) and 17 mL of dry iPrOH (Sigma Aldrich ©) were mixed in order to get a 0.15 M solution in a glove box, and it was stirred and heated in the glove box at 70ºC for 20 minutes. Then, the mp-TiO2 coated substrates were immersed in the solution at 70ºC for 20 minutes and the substrates were rinsed with iPrOH. Afterwards, substrates were heated up at 435ºC for 30 minutes.

The methylammonium iodide was synthesized as described previously.[36]

For the perovskite deposition, a 3:1 molar ratio solution of methylammonium iodide and $PbCl_2$ (Sigma Aldrich © 98%) in DMF (dimethyl formamide) was prepared. The perovskite precursor was deposited by spin-coating over the mp-TiO_2 layer at 2000 rpm for 1 min. The as-deposited substrates were heated at 120ºC for 30 minutes, and their colour changed from yellow to black.

The spiro-OMeTAD (1-Material ©), the HTM, was dissolved in chlorobenzene (CBZ) to reach a 70 mg/mL. Also, 28.8 µl of tBuPyr (tert-butylpyridine) and 17.5 µl of a 520 mg/mL of a LiTFSI solution in acetonitrile were added to the OMeTAD solution as additives. The HTM layer was deposited by spin-coating the solution onto the perovskite at 2000 rpm for 1 minute.

Finally, 80 nm of gold metal was evaporated as the anode by thermal evaporation at a pressure not higher than $1x10^{-6}$ mbar.

All the steps for the alumina coating and the perovskite and HTM deposition were carried out inside the glove box to avoid humidity ([O2] < 100 ppm and [H2O] < 0.1 ppm).

Current vs voltage (JV) measurements.

The solar cells performances were measured with a Sun 200 solar simulator (150 W, ABET Technologies) with the appropriate filters to simulate the AM 1.5G solar spectrum. A silicon diode was used to set the illumination intensity to $100mWm^{-2}$. The applied potential and cell current were measured with a Keithley © 2400 digital source meter.

Time Resolved Photo-induced measurements.

All photo-induced measurement techniques such as PICE (Photo-induced charge extraction, PIT-PV (photo-induced transient Photovoltage), PIT-PC (photo-induced transient photocurrent) and PIDC (photo-induced differential charging) are described with system diagrams at the Supplementary Information.

Results and Discussion.

Device characterization.

Figure 1 illustrates the current density *vs* voltage measurements (IV curves) for archetypal MAPI perovskite solar cells and the Al_2O_3 coated ones under standard sun-simulated irradiation condition ($100mW/cm^2$ @1.5 AM G).

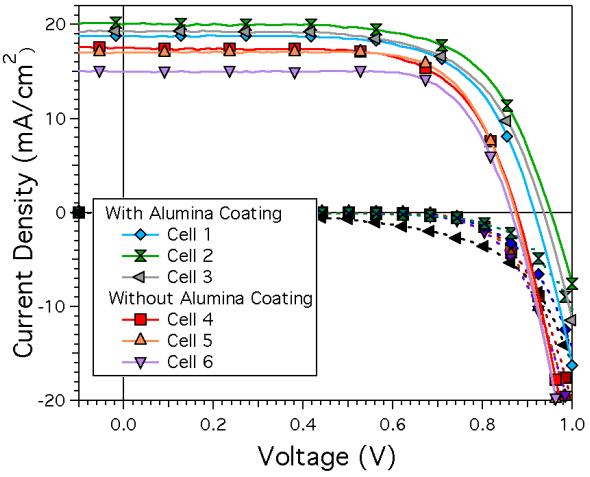

Figure 1. Several MAPI perovskite solar cells with and without the Al2O3 modified mp-TiO2/MAPI interface under 1 sun illumination and the corresponding dark curves (dashed lines).

As can be seen in Figure 1, solar cells using Al_2O_3 mp-TiO_2 coated MAPI perovskite solar cells show an increase in Voc and photocurrent leading to an average efficiency of η_{Al2O3}=12% in contrast to standard MAPI perovskite solar cell that show a standard average efficiency of η=10.2%. Table 1 lists all the relevant parameters for the measured cells in this work.

Table 1. Most relevant parameters obtained from the IV curves illustrated in Figure 1.

Device number	Voc (mV)	Jsc (mA/cm2)	FF(%)[1]	η	Al2O3 coated
Cell 1	920	18.6	67.8	11.6	yes
Cell 2	960	20.1	66.1	12.7	yes
Cell 3	939	19.3	65.1	11.8	yes
Cell 4	870	17.6	67.9	10.4	no
Cell 5	870	17.0	72.3	10.7	no
Cell 6	860	15.0	73.6	9.5	no

[1]device fill factor. Solar cell area of $0.25cm^2$. All solar cells were fabricated and measured under the same conditions at forward bias.

Further measurements of solar cells (Figure 2) fabricated in different days and conditions, as the devices depicted and listed in Figure 1 and Table 1 respectively, but always keeping identical measurement and fabrication conditions within each set of samples of Al_2O_3 coated mp-TiO_2 and the corresponding MAPI perovskite solar cells as control show identical trend with the Al_2O_3 modified mp-TiO2/MAPI interface having higher Voc and, in average, higher solar-to-energy conversion efficiency.

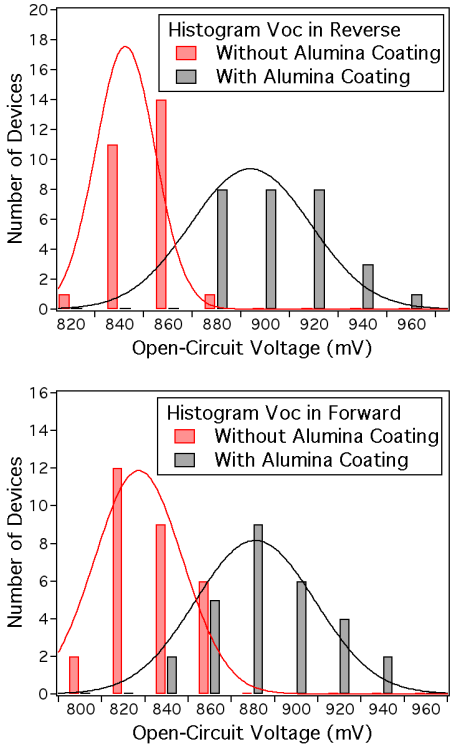

Figure 2. Solar cell open-circuit voltage (Voc) distribution for 28 Al_2O_3 coated mp-TiO_2 devices (grey) and 27 MAPI perovskite solar cells (red). Top, devices measured under reverse bias. Bottom, devices measured under forward bias.

In order to understand the effect of the Al_2O_3 onto the mp-TiO_2 and the overall solar cell performance and compare to what has been observed in DSSC we have carried out different experiments detailed below. The use of photo-induced differential charging (PIDC) has been very useful to analyse the accumulated charge at the solar cell under different light-bias (solar cell voltage induced by different illumination intensities) in DSSC[37], QDSC[38], OSC[39] and more recently in MAPI solar cells[16]. Moreover, it allows comparing the photo-generated charge density, at the same Voc, for different solar cells and, furthermore, is a key measurement in order to fairly compare charge recombination lifetime between different types of solar cells.

Photo-Induced Differential Charging (PIDC).

The details for the PIDC technique can be found at the Supplementary information of this manuscript. In brief, the charge is measured using PIT-PV and PIT-PC (photo-induced transient photo-current) as our group and others have previously demonstrated[40]. The use of PIDC is particularly necessary when the PICE decay has a longer lifetime than the measured PIT-PV decay at 1 sun (as for MAPI perovskite solar cells in Figure 3).

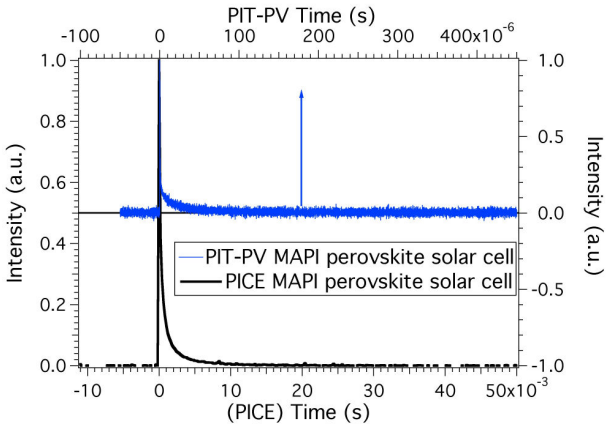

Figure 3. PICE decay (black line) for a MAPI perovskite solar cell and the PIT-PV transient (blue line) upon sun-simulated illumination equivalent to 1 sun. Notice the different time scales for the PICE (bottom axis) and the PIT-PV (top axis).

To estimate the photo-generated charge stored at the MAPI perovskite solar cell we must assume that (a) the solar cell has not charge losses at short circuit and (b) the PIT-PC under 1 sun and in the dark are similar. In other words, the charge generation efficiency is similar at short-circuit and at open circuit solar cell conditions. Figure 4 shows the PIT-PC measurements for both types of MAPI perovskite solar cells.

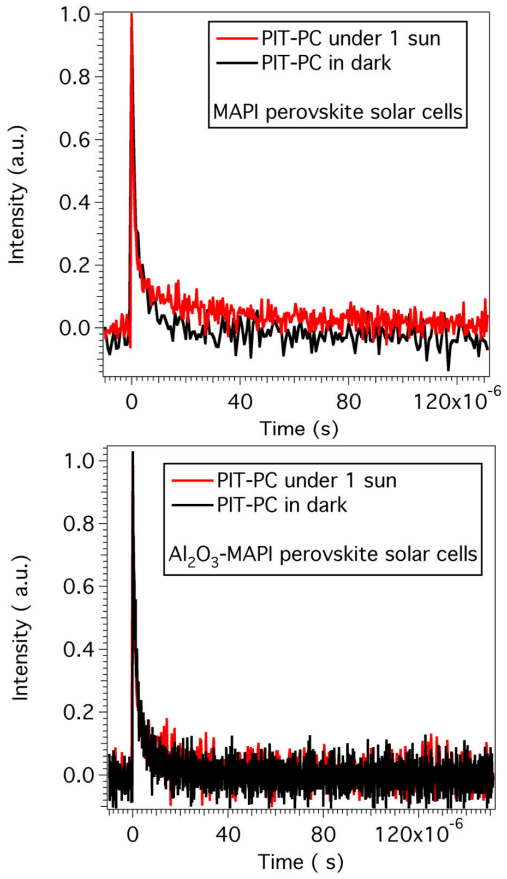

Figure 4. PIT-PC decays measured for (top) mpTiO2/MAPI perovskite and (bottom) Al2O3/mpTiO2/ MAPI perovskite solar cells.

As can be seen in Figure 4, either the PIT-PC under 1 sun or under dark for both type of solar cells are quite close. Hence, we carried out the PIDC for both type of solar cell devices. Figure 5 illustrates the charge measured from the PIDC vs solar cell voltage.

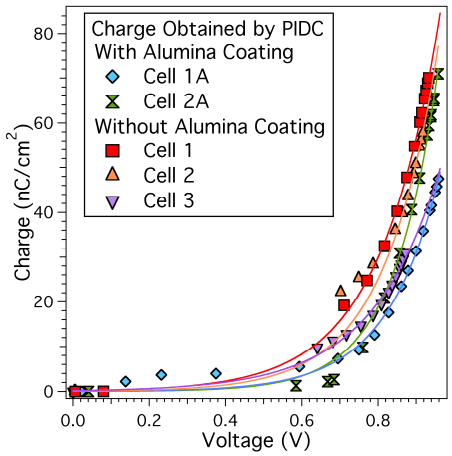

Figure 5. Measured charge using PIDC at different solar cell voltage from MAPI perovskite solar cells and Al2O3–coated perovskite solar cells. The Cell 3A has been removed for clarity read-out of the data in the figure.

In contrast to previous measurements on DSSC with the Al_2O_3 coating, there is no sensible and reproducible shift between the measured exponential curves[41]. In DSSC with the mp-TiO_2 conformally coated with Al_2O_3 a shift of the measured charge vs voltage exponential curve is observed and assigned to a shift of the TiO_2 conduction band edge with concomitant shift of the quasi-Fermi level for the electrons at the mp-TiO_2. The mp-TiO_2 conduction band shift plus the measured slower interfacial recombination kinetics between the electrons at the mp-TiO_2 and the oxidized electrolyte, in DSSC, lead to a measured increase in the open circuit voltage of the DSSC. Thus, next is to measure the PIT-PV in the MAPI perovskite solar cells and see if there is correlation with the measured higher open circuit voltage.

Photo-Induced Transient Photovoltage (PIT-PV).

The PIT-PV technique has been widely used to correlate the measured charge, at a given voltage, with the charge recombination lifetime. In a seminal paper[42], Bisquert and Zaban defined the Voc decay technique for DSSC and later our group and others used a modified version of the technique (see Supplementary Information), which is based in small perturbation of the open-circuit cell voltage using a fast light pulse. The fast pulse disrupts the equilibrium raising the quasi-Fermi level for the electrons at the mp-TiO_2, which is restored after the pulse finishes to the original energy level and, thus, restoring the initial open-circuit voltage. In DSSC, the voltage decay promoted by the fast light pulse results in a mono-exponential decay with an amplitude always smaller than 10mV to ensure a minor perturbation of the cell open-circuit voltage.

Figure 6 illustrates the PIT-PV decays for our MAPI perovskite solar cells.

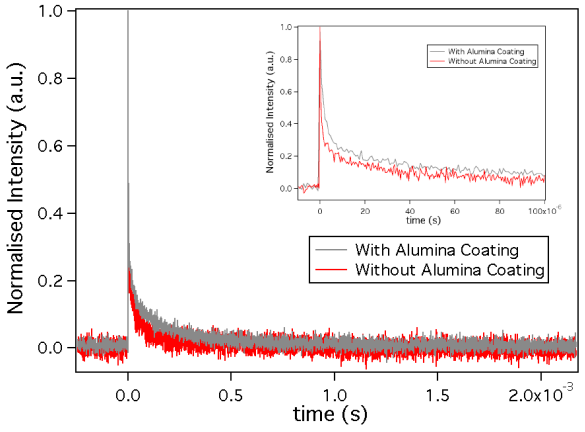

Figure 6. Measured PIT-PV for a MAPI perovskite solar cell (black) and an Al_2O_3-coated MAPI perovskite solar cell (red) at 100mW/cm² light irradiation. The inset shows the fastest component of the PIT-PV.

The first difference observed in comparison to the PIT-PV decays in DSSC is the bi-exponential nature of the decays measured either with the Al_2O_3 coating or the MAPI perovskite as control. As shown in Figure 6 both samples show bi-exponential decays with τ_1 = 175 μs (20%) and $\tau 2$= 3 μs (80%) for Al_2O_3 coated solar cells and τ_1= 73μs (20%) and τ_2= 0.8 μs (80%) for MAPI perovskite solar cells

under similar charge density ~35nC/cm^2. This result is in good agreement with previous data[16, 23].

In MAPI perovskite solar cells, there is still far from clear the origin of the large photo-voltage measured that in some cases is overpassing 1V. Moreover, the large differences in charge density measured using PICE (see Supplementary Information) and PIDC and the different chemical nature that both types of charges may have, tking into account the differences in the kinetics from the bi-exponential PIT-PV decay, makes even more challenging to assign the processes that gives rise to the accumulated charges measured. Thus, it may well be that the measured transient photo-voltage does not correspond to a charge recombination process (charge losses) but to, for example, a reorganization of dipoles at the MAPI that leads to a change in voltage or to a combination of both processes. Nevertheless, we have studied in detail the PIT-PV and we have proposed that the fast component of the PIT-PV decay is the product of the electron-hole recombination process and hence the photo-induced charge recombination lifetime[16]. Hence, based in our past experience we have also used for comparison purposes between MAPI solar cells the charge measured by PIDC and the fastest component of the PIT-PV decay.

Charge recombination lifetime vs charge density.

It is important to notice that , for the comparison, we use the measured charge from PIDC, instead of the measured cell Voc at different light intensities (so called light bias) because it is well established for other solar cells such as DSSC, OPV and QDSC that it may well be that at the same Voc different solar cells have very different amount of stored charge and thus, the compared charge recombination lifetime will not be meaningful and appropriate. Figure 7 illustrates the carrier recombination lifetime vs electrical charge for both type of solar cells.

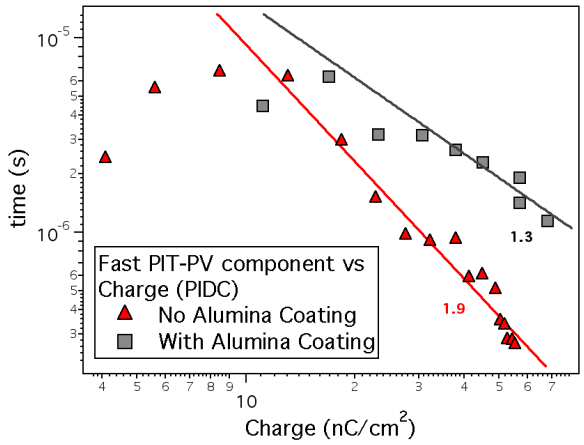

Figure 7. Non-radiate carrier recombination lifetime (fast component PIT-PV decay) vs solar cell electrical charge measured by PIDC. The numbers correspond to the recombination order factor (OF)

As illustrated in Figure 7 the use of Al_2O_3 conformal coating leads to slower interfacial charge recombination lifetimes when compared to the standard mpTiO_2 film.

We also would like to emphasize that although the slowest component of the PIT-PV decay, either with the charge measured using PICE or the charge measured using PIDC, cannot reproduce fairly the J_{rec} (data shown in the Supplementary Information, Table S1) and, thus, seems that is not related to the "*electrical charge*" (understanding as *electrical charge* electrons and holes) at the MAPI perovskite still accounts for at least 20% of the PIT-PV decay and, interestingly the PIT-PV slow component of the decay is slower for Al_2O_3 . A comparison of both types of solar cells, the Al_2O_3 coated and the MAPI perovskite device, is illustrated in Figure 8.

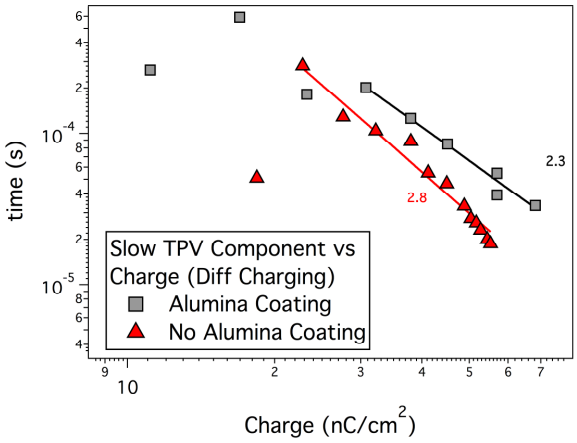

Figure 8. The slow component for the PIT-PV decays vs solar cell measured charge by PIDC at different light bias. The numbers correspond to the recombination order factor (OF)

Conclusions

We have used Al_2O_3 conformal coating from solution-processed methods onto mesoporous TiO_2 electrodes (mpTiO_2) used in the preparation of efficient MAPI perovskite solar cells. The use of Al_2O_3 coating leads to an improvement in the solar cell efficiency mainly due to a higher open circuit voltage (Voc). The increase in Voc is systematic and reproducible. Moreover, we have studied the interfacial charge recombination processes using photo-induced time resolved methods in complete devices under sun-simulated irradiation conditions. Using PIDC we have not observed a clear shift on the exponential charge distribution as it was demonstrated for Al_2O_3/mpTiO_2 coated DSSC.

The analysis of the PIT-PV decays shows two different time components, in good agreement with previous measurements with other MAPI perovskite solar cells. In fact, for Al_2O_3 coated solar cells both time components present at the PIT-PV decay are slower in comparison with the standard MAPI perovskite solar cell. A careful comparison of both charge recombination lifetime components at the same charge density further confirms that the recombination lifetime for Al_2O_3 treated solar cells is significantly slower.

Hence, it seems clear that the slower charge recombination kinetics in the Al_2O_3 coated MAPI perovskite solar cells can be directly correlated with the solar cell Voc improvement. However, unlike the case of DSSC, it was unclear why both PIT-PV time components are affected by

the presence of the Al_2O_3 coating onto the mesoporous TiO_2. A feasible hypothesis in the light of the results obtained in this work is that both PIT-PV components can be assigned to two different charge recombination processes; one process related to the charge transfer of electrons from the TiO_2, upon electron transfer from the MAPI perovskite under illumination, with the holes at the HTM and a second, and faster charge recombination process, between electrons at the TiO_2 and holes at the MAPI perovskite. In both cases the Al_2O_3 will act as a physical barrier (alike in the case of DSSC) decreasing the rate of the back electron transfer reaction upon photo-induced electron injection from the MAPI perovskite to the TiO_2 CB.

Acknowledgements.

The authors would like to thank ICIQ and ICREA for the economical support and the Spanish MINECO for projects CTQ2013-47183-R and the Severo Ochoa Excellence Accreditation 2014.2018(SEV-2103-0319).

ASSOCIATED CONTENT

Supporting information contains PICE, voltage stability and PIT-PV measurement. A detailed description of the PICE and PIT-PV systems and, moreover, a HRTEM image of the coated and uncoated Al_2O_3 nanoparticles. This material is available free of charge via the Internet at http://pubs.acs.org.

AUTHOR INFORMATION

Corresponding Author

*epalomares@iciq.es

Author Contributions

The manuscript was written through contributions of all authors. All authors have given approval to the final version of the manuscript.

References

1. Park, N.-G., Perovskite solar cells: an emerging photovoltaic technology. Mater. Today. **2014**, 18, (2), 65-72.
2. Mali, S. S.; Shim, C. S.; Patil, P. S.; Hong, C. K., Once again, organometallic tri-halide perovskites. Mater. Today. **2015**, 18, (3), 172-173.
3. Green, M. A.; Ho-Baillie, A.; Snaith, H. J., The emergence of perovskite solar cells. Nat Photonics. **2014**, 8, (7), 506-514.
4. Kojima, A.; Teshima, K.; Shirai, Y.; Miyasaka, T., Organometal Halide Perovskites as Visible-Light Sensitizers for Photovoltaic Cells. J. Am. Chem. Am. **2009**, 131, (17), 6050-6051.
5. Yang, W. S.; Noh, J. H.; Jeon, N. J.; Kim, Y. C.; Ryu, S.; Seo, J.; Seok, S. I., High-performance photovoltaic perovskite layers fabricated through intramolecular exchange. Science **2015**, 348, (6240), 1234-1237.
6. Mathew, S.; Yella, A.; Gao, P.; Humphry-Baker, R.; CurchodBasile, F. E.; Ashari-Astani, N.; Tavernelli, I.; Rothlisberger, U.; NazeeruddinMd, K.; Gratzel, M., Dye-sensitized solar cells with 13% efficiency achieved through the molecular engineering of porphyrin sensitizers. Nat. Chemistry **2014**, 6, (3), 242-247.
7. Kan, B.; Li, M.; Zhang, Q.; Liu, F.; Wan, X.; Wang, Y.; Ni, W.; Long, G.; Yang, X.; Feng, H.; Zuo, Y.; Zhang, M.; Huang, F.; Cao, Y.; Russell, T. P.; Chen, Y., A Series of Simple Oligomer-like Small Molecules Based on Oligothiophenes for Solution-Processed Solar Cells with High Efficiency. Journal of the American Chemical Society. **2015**, 137, (11), 3886-3893.
8. Chuang, C.-H. M.; Brown, P. R.; Bulovic, V.; Bawendi, M. G., Improved performance and stability in quantum¬†dot solar cells through band alignment¬†engineering. Nat Materials **2014**, 13, (8), 796-801.
9. Tan, Z.-K.; Moghaddam, R. S.; Lai, M. L.; Docampo, P.; Higler, R.; Deschler, F.; Price, M.; Sadhanala, A.; Pazos, L. M.; Credgington, D.; Hanusch, F.; Bein, T.; Snaith, H. J.; Friend, R. H., Bright light-emitting diodes based on organometal halide perovskite. Nat Nanotechnology **2014**, 9, (9), 687-692.
10. Kim, H.-S.; Mora-Sero, I.; Gonzalez-Pedro, V.; Fabregat-Santiago, F.; Juarez-Perez, E. J.; Park, N.-G.; Bisquert, J., Mechanism of carrier accumulation in perovskite thin-absorber solar cells. Nat Communications **2013**, 4, (2242), 1-7
11. Unger, E. L.; Hoke, E. T.; Bailie, C. D.; Nguyen, W. H.; Bowring, A. R.; Heumuller, T.; Christoforo, M. G.; McGehee, M. D., Hysteresis and transient behavior in current-voltage measurements of hybrid-perovskite absorber solar cells. Energy Environ. Sci. **2014**, 7, (11), 3690-3698.
12. Tress, W.; Marinova, N.; Moehl, T.; Zakeeruddin, S. M.; Nazeeruddin, M. K.; Gratzel, M., Understanding the rate-dependent J-V hysteresis, slow time component, and aging in CH3NH3PbI3 perovskite solar cells: the role of a compensated electric field. Energy Environ. Sci. **2015**, 8, (3), 995-1004.
13. Sanchez, R. S.; Gonzalez-Pedro, V.; Lee, J.-W.; Park, N.-G.; Kang, Y. S.; Mora-Sero, I.; Bisquert, J., Slow Dynamic Processes in Lead Halide Perovskite Solar Cells. Characteristic Times and Hysteresis. J. Phys. Chem. Lett. **2014**, 5, (13), 2357-2363.
14. Gottesman, R.; Haltzi, E.; Gouda, L.; Tirosh, S.; Bouhadana, Y.; Zaban, A.; Mosconi, E.; De Angelis, F., Extremely Slow Photoconductivity Response of CH3NH3PbI3 Perovskites Suggesting Structural Changes under Working Conditions. J. Phys. Chem. Lett. **2014**, 5, (15), 2662-2669.
15. Marin-Beloqui, J. M.; Hernandez, J. P.; Palomares, E., Photo-induced charge recombination kinetics in MAPbI3-xClx perovskite-like solar cells using low band-gap polymers as hole conductors. Chem. Commun. **2014**, 50, (93), 14566-14569.
16. O'Regan, B. C.; Barnes, P. R. F.; Li, X.; Law, C.; Palomares, E.; Marin-Beloqui, J. M., Optoelectronic Studies of Methylammonium Lead Iodide Perovskite Solar Cells with Mesoporous TiO2: Separation of Electronic and Chemical Charge Storage, Understanding Two Recombination Lifetimes, and the Evolution of Band Offsets during J‚ÄìV Hysteresis. J. Am. Chem. Soc. **2015**, 137, (15), 5087-5099.
17. Wu, X.; Yu, H.; Li, L.; Wang, F.; Xu, H.; Zhao, N., Composition-Dependent Light-Induced Dipole Moment Change in Organometal Halide Perovskites. J. Phys. Chem. C **2015**, 119, (2), 1253-1259.
18. Mosconi, E.; Quarti, C.; Ivanovska, T.; Ruani, G.; De Angelis, F., Structural and electronic properties of organo-halide lead perovskites: a combined IR-spectroscopy and ab initio molecular dynamics investigation. Phys. Chem. Chem. Phys. **2014**, 16, (30), 16137-16144.
19. Green, M. A.; Emery, K.; Hishikawa, Y.; Warta, W.; Dunlop, E. D., Solar cell efficiency tables (Version 45). Progress Photovol. **2015**, 23, (1), 1-9.
20. Marchioro, A.; Teuscher, J.; Friedrich, D.; Kunst, M.; van de Krol, R.; Moehl, T.; Gratzel, M.; Moser, J.-E., Unravelling the mechanism of photoinduced charge transfer processes in lead iodide perovskite solar cells. Nat Photonics **2014**, 8, (3), 250-255.
21. Gonzalez-Pedro, V.; Juarez-Perez, E. J.; Arsyad, W.-S.; Barea, E. M.; Fabregat-Santiago, F.; Mora-Sero, I.; Bisquert, J., General Working Principles of CH3NH3PbX3 Perovskite Solar Cells. Nano Lett. **2014**, 14, (2), 888-893.
22. Manser, J. S.; Kamat, P. V., Band filling with free charge carriers in organometal halide perovskites. Nat Photonics **2014,** 8, (9), 737-743.

23. Roiati, V.; Colella, S.; Lerario, G.; De Marco, L.; Rizzo, A.; Listorti, A.; Gigli, G., Investigating charge dynamics in halide perovskite-sensitized mesostructured solar cells. Energy Environ. Sci. 2014, 7, (6), 1889-1894.

24. deQuilettes, D. W.; Vorpahl, S. M.; Stranks, S. D.; Nagaoka, H.; Eperon, G. E.; Ziffer, M. E.; Snaith, H. J.; Ginger, D. S., Impact of microstructure on local carrier lifetime in perovskite solar cells. Science **2015**, 348, (6235), 683-686.

25. Eperon, G. E.; Stranks, S. D.; Menelaou, C.; Johnston, M. B.; Herz, L. M.; Snaith, H. J., Formamidinium lead trihalide: a broadly tunable perovskite for efficient planar heterojunction solar cells. Energy Environ. Sci. **2014**, 7, (3), 982-988.

26. Mei, A.; Li, X.; Liu, L.; Ku, Z.; Liu, T.; Rong, Y.; Xu, M.; Hu, M.; Chen, J.; Yang, Y.; Gratzel, M.; Han, H., A hole-conductor,Äìfree, fully printable mesoscopic perovskite solar cell with high stability. Science **2014**, 345, (6194), 295-298.

27. Liu, D.; Kelly, T. L., Perovskite solar cells with a planar heterojunction structure prepared using room-temperature solution processing techniques. Nat Photonics **2014**, 8, (2), 133-138.

28. Roldan-Carmona, C.; Malinkiewicz, O.; Soriano, A.; Minguez Espallargas, G.; Garcia, A.; Reinecke, P.; Kroyer, T.; Dar, M. I.; Nazeeruddin, M. K.; Bolink, H. J., Flexible high efficiency perovskite solar cells. Energy Environ. Sci. **2014**, 7, (3), 994-997.

29. Cabau, L.; Vijay Kumar, C.; Moncho, A.; Clifford, J. N.; Lopez, N.; Palomares, E., A single atom change "switches-on" the solar-to-energy conversion efficiency of Zn-porphyrin based dye sensitized solar cells to 10.5%. Energy Environ. Sci. **2015**, 8, (4), 1368-1375.

30. Reynal, A.; Forneli, A.; Martinez-Ferrero, E.; Antonio, S.-D.; Vidal-Ferran, A.; O'Regan, B. C.; Palomares, E., Interfacial Charge Recombination Between e-TiO2 and the I-/I3- Electrolyte in Ruthenium Heteroleptic Complexes: Dye Molecular Structure vs Open Circuit Voltage Relationship. J. Am. Chem. Soc. **2008**, 130, (41), 13558-13567

31. Yao, Z.; Wu, H.; Ren, Y.; Guo, Y.; Wang, P., A structurally simple perylene dye with ethynylbenzothiadiazole-benzoic acid as the electron acceptor achieves an over 10% power conversion efficiency. Energy Environ. Sci. **2015**, 8, (5), 1438-1442.

32. Palomares, E.; Clifford, J. N.; Haque, S. A.; Lutz, T.; Durrant, J. R., Control of Charge Recombination Dynamics in Dye Sensitized Solar Cells by the Use of Conformally Deposited Metal Oxide Blocking Layers. J. Am. Chem. Soc. **2003**, 125, (2), 475-482.

33. Palomares, E.; Clifford, J. N.; Haque, S. A.; Lutz, T.; Durrant, J. R., Slow charge recombination in dye-sensitised solar cells (DSSC) using Al2O3 coated nanoporous TiO2 films. Chem. Commun. **2002**, (14), 1464-1465.

34. Liu, Z.; Pan, K.; Liu, M.; Wang, M.; Lü, Q.; Li, J.; Bai, Y.; Li, T., Al2O3-coated SnO2/TiO2 composite electrode for the dye-sensitized solar cell. Electrochim. Acta **2005**, 50, (13), 2583-2589.

35. Han, G. S.; Chung, H. S.; Kim, B. J.; Kim, D. H.; Lee, J. W.; Swain, B. S.; Mahmood, K.; Yoo, J. S.; Park, N.-G.; Lee, J. H.; Jung, H. S., Retarding charge recombination in perovskite solar cells using ultrathin MgO-coated TiO2 nanoparticulate films. J. Mat. Chem. A **2015**, 3, (17), 9160-9164.

36. Im, J.-H.; Lee, C.-R.; Lee, J.-W.; Park, S.-W.; Park, N.-G., 6.5% efficient perovskite quantum-dot-sensitized solar cell. Nanoscale **2011**, 3, (10), 4088-4093.

37. Barnes, P. R. F.; Miettunen, K.; Li, X.; Anderson, A. Y.; Bessho, T.; Gratzel, M.; O'Regan, B. C., Interpretation of Optoelectronic Transient and Charge Extraction Measurements in Dye-Sensitized Solar Cells. Adv. Mater. **2013**, 25, (13), 1881-1922.

38. Albero, J.; Riente, P.; Clifford, J. N.; Pericàs, M. A.; Palomares, E., Improving CdSe Quantum Dot/Polymer Solar Cell Efficiency Through the Covalent Functionalization of Quantum Dots: Implications in the Device Recombination Kinetics. J. Phys. Chem. C **2013**, 117, (26), 13374-13381.

39. Shuttle, C. G.; Maurano, A.; Hamilton, R.; O'Regan, B. C.; de Mello, J. C.; Durrant, J. R., Charge extraction analysis of charge carrier densities in a polythiophene/fullerene solar cell: Analysis of the origin of the device dark current. Appl. Phys. Lett. **2008**, 93, (18), 183501.

40. Maurano, A.; Shuttle, C. G.; Hamilton, R.; Ballantyne, A. M.; Nelson, J.; Zhang, W.; Heeney, M.; Durrant, J. R., Transient Optoelectronic Analysis of Charge Carrier Losses in a Selenophene/Fullerene Blend Solar Cell. J. Phys. Chem. C **2011**, 115, (13), 5947-5957.

41. O'Regan, B. C.; Scully, S.; Mayer, A. C.; Palomares, E.; Durrant, J., The Effect of Al2O3 Barrier Layers in TiO2/Dye/CuSCN Photovoltaic Cells Explored by Recombination and DOS Characterization Using Transient Photovoltage Measurements. J. Phys. Chem. B **2005**, 109, (10), 4616-4623.

42. Bisquert, J.; Zaban, A.; Greenshtein, M.; Mora-Seró, I., Determination of Rate Constants for Charge Transfer and the Distribution of Semiconductor and Electrolyte Electronic Energy Levels in Dye-Sensitized Solar Cells by Open-Circuit Photovoltage Decay Method .J. Am. Chem. Soc. **2004**, 126, (41), 13550-13559.